Preprints.org

Article

Economical Experimental Device for Evaluating Thermal Conductivity in Construction Materials under Limited Research Funding

Damien Ali Hamada FAKRA [*] , Rijalalaina RAKOTOSAONA , Marie Hanitriniaina RATSIMBA ,
Mino Patricia RANDRIANARISON , Riad Benelmir

Article

Economical Experimental Device for Evaluating Thermal Conductivity in Construction Materials under Limited Research Funding

Damien Ali Hamada Fakra [1,2,†,‡,*] 🔾 **, Rijalalaina Rakotosaona** [2,‡] **, Marie Hanitriniaina Ratsimba** [2,‡] **, Mino Patricia Randrianarison** [2,‡] **and Riad Benelmir** [1,†]

[1]   University of Lorraine, Sciences and Technologies Faculty of Nancy, Campus Aiguillettes - BP 70239 / 54506 Vandoeuvre-Les-Nancy (FRANCE)

[2]   University of Antananarivo, Higher Polytechnic School of Antananarivo, Sis Ambihitsaina BP 1500 Antananarivo 101 (MADAGASCAR)

[*]   Correspondence: damien.fakra@univ-lorraine.fr or damien.fakra@univ-antananarivo.mg; Tel.: +33-7-8111-3532 (D.F.)

[†]   Current address 1: Laboratory for Studies and Research on Wood Materials (LERMAB), University of Lorraine

[‡]   Current address 2: Research Laboratory of Material, Process and Civil Engineering (LRMPGC), University of Antananarivo

Abstract: African scientific research faces formidable challenges, particularly with limited access to state-of-the-art measurement instruments. The high cost associated with these devices presents a significant barrier for regional research laboratories, impeding their ability to conduct sophisticated experiments and gather precise data. This predicament not only hampers the individual laboratories but also has broader implications for the African scientific community and the advancement of knowledge in developing nations—the financial cost barrier considerably impacts the research quality of these laboratories. Reflection on technical and economical solutions needs to be quickly found to help these countries advance their research. In civil Engineering, the thermal conductivity property is the most important measurement for characterising heat transfer in construction materials. Existing devices (i.e., conductometers) in a laboratory are expensive (approximately 30,000 euros) and unavailable for some African laboratories. The study proposes a new and affordable device to evaluate thermal conductivity in construction materials. The method involves establishing a thermal flux between a heat source (from the Joule effect provided by steel wool where a current is circulating) and a cold source (generated by ice cube) under steady-state conditions. The development of the cylindrical prototype is based on the comparative flux-meter method outlined in the measuring protocol of the ASTM E1225 standard document. Experiments were conducted on four distinct materials (polystyrene, wood, agglomerated wood, and rigid foam). The results indicate a correct correlation between the experimental values obtained from the newly developed prototype and the reference values found in the literature. For example, concerning the experimental polystyrene study, the detailed case analysis reveals a good correlation, with a deviation of only 4%. The percent error found falls within the acceptable range indicated by the standards recommendations of the ASTM E1225 standard, i.e., within 5% acceptable error.

Keywords: construction; low-tech; low-cost; conductivity; thermal transfer; steady state

1. Introduction

The measurement of thermal conductivity [1] in building envelopes has been the subject of a multitude of studies, encompassing both steady-state [2] and dynamic (refer to [2–4]) conditions. The investigations are classified according to whether they are performed in situ [5] on actual walls or in laboratory settings utilizing samples (see [6–8]). A multitude of methodologies are accessible in the scientific community, as evidenced by the following techniques: Heat Flow Meter (HFM) (refer to [9–12]), Transient-Cylinder Bridge Heat Flow Meter (TCB-HFM) method [13], Infrared Thermography (IRT) method ([14–20]), Transient Plane Source (TPS) method [21], Guarded Hot Flux (GHF) method [22], Guarded Hot Plate (GHP) method [23], Guarded Hot Box (GHB) method [24], and Surface Heat Balance (SHB) method (refer to [25,26]). Due to the abundance of these methods, some researchers have compared them to determine the most dependable. As an illustration, Osasu et al. [27] performed

comparative analyses of two experimental characterization methods (the DT-25 and the Hot Box test) for polypropylene material. In the interim, Manzena et al. [28] tried to introduce a novel calorimeter that could measure the thermal conductivity of a porous building material at an affordable cost. In their study, Behman et al. [29] introduced an innovative approach for acquiring empirical data regarding the thermal properties of a structure's environment, such as its thermal conductivity. Nevertheless, these devices are frequently unaffordable in price. For example, TESTO provides various measuring instruments priced within the range of 570 to 1032 euros (see [30–32]). A. Ricklefs et al. [33]introduced a method in 2017 for determining the thermal conductivity of a Change Phase Material (CPM) within innovative materials. In contrast, Lucchi et al. [34]conducted a comparative analysis of various benchmarks for quantifying thermal characteristics in heterogeneous substances. Antonio Gagliano et al. [35] established a relatively straightforward and economical experimentation for determining the thermal conductivity of a "green roof" material across varying moisture conditions. The work of Gagliano et al. is the most recent development in the field. The thermal conductivity measurement in innovative construction materials poses a twofold challenge with scientific and financial implications. Across each continent, there is a growing emphasis on sustainable development and the construction of energy-efficient buildings to meet the needs of rapidly urbanizing populations. This drive has spurred the exploration and adoption of innovative construction materials with improved thermal properties to mitigate energy consumption and enhance indoor comfort. However, accurately assessing the thermal conductivity of these materials remains a critical hurdle. Understanding how these materials interact with varying climatic conditions prevalent in different regions of these countries is essential for their effective deployment. Financially, investments in research and development to measure the thermal properties of these innovative materials can be substantial, particularly in resource-constrained settings. So, These developing countries need to address the scientific intricacies and financial constraints inherent in measuring the thermal conductivity of innovative construction materials. Measurements of thermal conductivities hold significant importance across various applications. Indeed, this thermophysical parameter finds relevance in diverse research domains, including the identification and categorization of scrap materials within the recycling sector [36], the utilization of low thermal conductivity materials in construction [37], and the enhancement of indoor comfort and energy efficiency in buildings [38], among others. Boudenne et al. [39], have devised an innovative method for measuring the conductivity of insulating materials. In this approach, a specimen whose conductivity is to be determined is sandwiched between two layers of a highly conductive material (see Figure 1). One of these layers, designated as the "front panel," houses a heating element. Conversely, the other layer, termed the "back face," is exposed to a surrounding more cold temperature. The experiment is conducted under transient conditions.
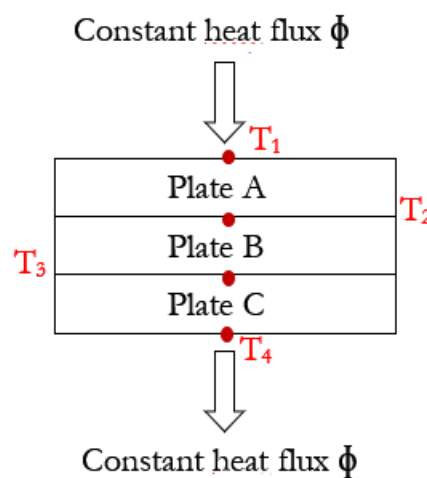

Figure 1. Schematic view of the experimental thermal exchange model ($T_1 > T_2 > T_3 > T_4$).

The scientific literature extensively documents research on the conductivity of composite materials (see [40,41]). These studies often involve materials that exhibit neither homogeneity nor isotropy, rendering them complex in nature. One way is to consider that the material generally has homogeneous properties. The conductivity of the composite material can then be approximated by an average value from the conductivities of the phases that compose it. In 2020, Fakra et al. [42] presented a low-cost and efficient solution for accurately determining the thermal conductivity of building materials. The simplicity of the measurement process using the new device named McM or MultiCoefMeter, along with the reliability and accuracy of the results, makes it a practical choice for researchers and practitioners in the field. The device's design allows for easy replication and modification for different translucent materials (see [43]). The device can support research and development efforts in building materials by providing a cost-effective and efficient method for characterizing the thermal properties of any construction material. In 2022, Delort et al. [44] detailed a study on the uncertainty assessment of the McM device. The uncertainty assessment conducted in the study of Delort et al. [44] was permitted to ensure the metrological traceability, accuracy, and reliability of measurement results obtained from the experimental device McM. In this study, we propose a rather a new and original device for measuring the thermal conductivity of complex materials that is more low-tech, more affordable, highly precise, and capable of meeting the research laboratory needs of developing countries.

2. Methodology

The methods employed to measure the thermal conductivity of materials vary based on the material's surface and the type of contact (fluid-solid or solid-solid) of the surface to be measured. This work uses the transient plane source (TPS) technique.

The measurement procedure involves sandwiching plate B, designated for study, between the two identical plates A and C (refer to Figure 2), both plates possessing known thermal conductivity λ_0. Subsequently, a constant flux (for instance, $T_1 > T_4$, with T_1 and T_4 being constant temperatures) is conducted through the three plates (refer to Figure 2). By measuring the temperatures of the outer walls of A and C (denoted as T_1 and T_4) along with the contact points of the sandwiched plate B (i.e., T_2 and T_3), it is possible to determine the thermal conductivity value of plate B. This determination is made utilizing the following relationship, which is grounded in the conservation of flux according to Fourier's law in steady-state conduction heat exchange:

$$\phi = \lambda_0 \, A_0 \, \frac{T_2 - T_1}{d_0} \; = \; \lambda_x \, A_x \, \frac{T_3 - T_2}{d_x} \; = \; \lambda_0 \, A_0 \, \frac{T_4 - T_3}{d_0} \tag{1}$$

From the relationship (1), we obtain:

$$\lambda_X = \lambda_0 \, \frac{A_0}{A_x} \, \frac{d_x}{d_0} \, \frac{T_2 - T_1}{T_3 - T_2} \tag{2}$$

where else,

$$\lambda_X = \lambda_0 \, \frac{A_0}{A_x} \, \frac{d_x}{d_0} \, \frac{T_4 - T_3}{T_3 - T_2} \tag{3}$$

Each relationship (i.e., (2) or (3)) can determine the thermal conductivity value λ_x.
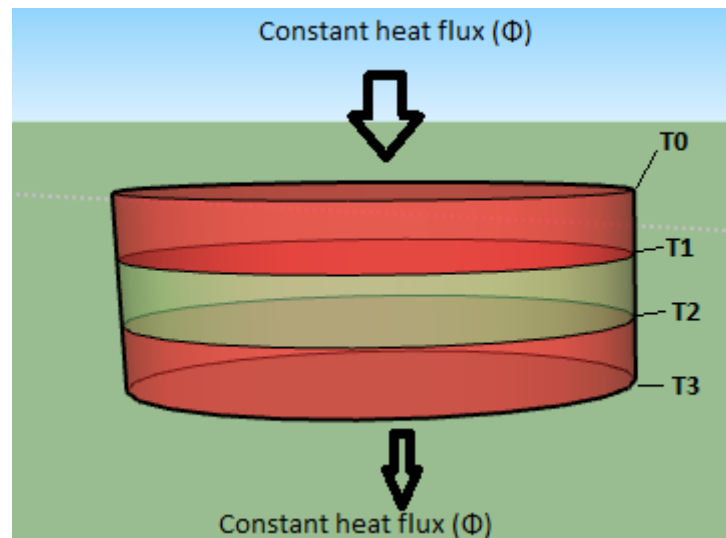
Figure 2. Heat transfer through a material sample with the TPS (Transient Plane Source) measurement technique.

3. Conception of the New Device (Step by Step)

The experimental setup proposed in this work respects the concept of eco-design, which entails reducing financial costs, employing low-technology approaches to manufacturing, ensuring environmental compatibility of the system, and garnering social acceptance of the device. The equipment utilized for the fabrication of the hot and cold sources, system insulation, and instrumenting of the apparatus is described in the subsequent section.

3.1. A Hot Source: Steel Wool

A piece of stainless steel wool (see Figure 3) was utilized to generate the hot heat source. The metal was wound to form a filament of specific thickness and length, as illustrated in Figure 4. Subsequently, an electric current passes through the filament to produce heat by the Joule effect.

Figure 3. Steel wool

A variable alternating current generator (see Figure 4) with a maximum intensity of 6 A and a maximum voltage of 10 V is connected between the two extremities of the filament. The thermal power produced by the filament is then deducted from the following formula:

$$P = U.I.Cos(\alpha) \tag{4}$$

$Cos(\alpha)$ is the power factor. There is no phase change in the active dissipative resistance of the filament. This induces a $\alpha = 0$ and thus a $cos(\alpha) = 1$.
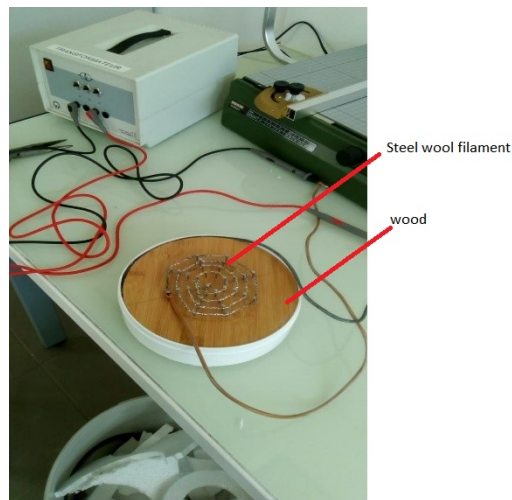

Figure 4. Hot source of the device made with a steel wool filament and current generator

The dimensions of the filament are as follows: 84 centimeters in length and 10 cm in diameter (around nails serving as supports).

3.2. Flat Steel Iron

Flat steel irons are employed to provide support for the material testing process. This technique serves three purposes:

- To ensure uniform thermal flux transfer across the entire surface of the test material. The sample diameter must match that of the flat steel iron (see Figure 5 for the dimension of the flat steel iron).
- To accelerate the heat transfer process between the two sample surfaces in contact with the cold and hot source of the device.
- To secure the sample from too high or too low temperatures from hot and cold heat sources of the device.
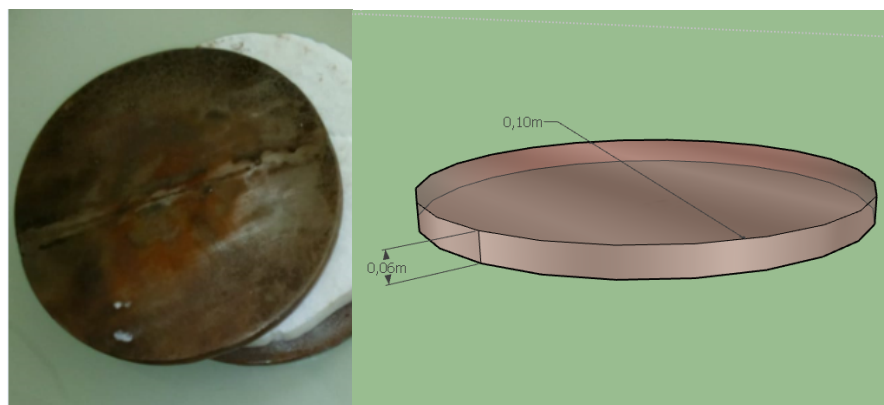

Figure 5. Flat steel iron

3.3. A Cold Source: The Ice Cubes

The ice cubes are hermetically isolated and represent the cold source of the device (see Figure 6). The isolation, utilized from polystyrène material, can keep the temperature of the ice cubes constant for ten hours (see the test realized in Figure 7 and 8 with infrared camera). The ice cubes are deposited in a cylindrical compartment of 0.157 cm^3 (see Figure 9).

3.4. The Adiabatic Part of the Device

The calorimeter is insulated with a 3.5 cm thick expanded polystyrene. The insulate is maintained by two PVC cylinders, one grey on the inside and one white on the outside, as depicted in Figure 9. The selection of materials for designing the compartment is economical and technically reliable. PVC, known for its low cost and minimal thermal conductivity ranging between 0.037 and 0.039 W^{-1}, is an excellent supplementary insulator alongside the affordable polystyrene, which also boasts excellent insulating properties. Consequently, radial flows (ϕ_{trans}) can be disregarded, and only the descending flows (ϕ_{desc}) from the heat source of our device, illustrated in the Figure 6, are considered in the measurement and the thermal conductivity value calculation.
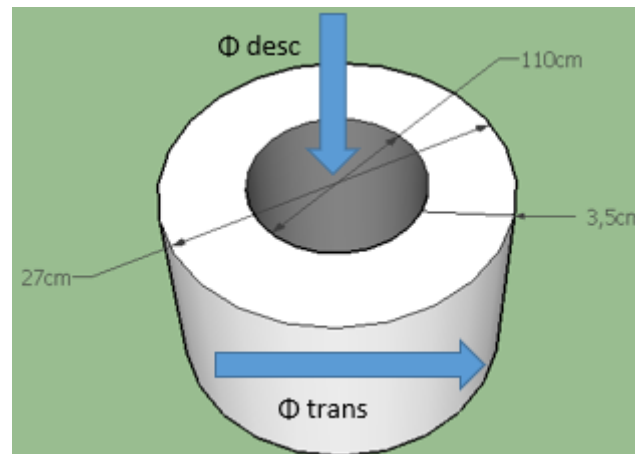

Figure 6. Visualization and dimensions of calorimeter thermal insulation

3.5. Calibration Tests and Measurement Protocol

Verification tests were conducted to assess the reliability of our cold and hot sources and measurement sensors. Subsequently, a protocol for measuring the thermal conductivity of samples utilizing the TPS technique was realized. All this work is described in this section.

3.5.1. Cold Source Verification Test

The exterior PVC is a small office waste bin measuring 18 cm in diameter, 27 cm in height, and 2 mm thick. Tests of the heat retention (cold and hot) of our sources have been carried out to ensure the duration of the maintenance of the temperature of each of them in the compartment. An infrared camera enabled these tests to be carried out. The test protocol consisted of thermal imaging of the device containing the source (either cold or hot) and its environment over a defined period. Figures 7 and 8 show the results obtained from the cold source test. The final result indicated that the source's temperature varied only one degree after 7 hours. This time is much longer than the time used to measure the thermal conductivity of our sample.
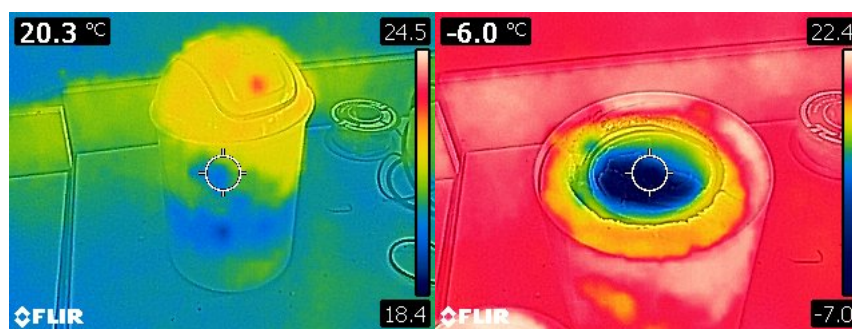

Figure 7. Temperature measurements inside and outside the small waste bin insulated at the beginning of the experiment. Figure left: heat flow from the outside. Figure Right: heat flow inside.
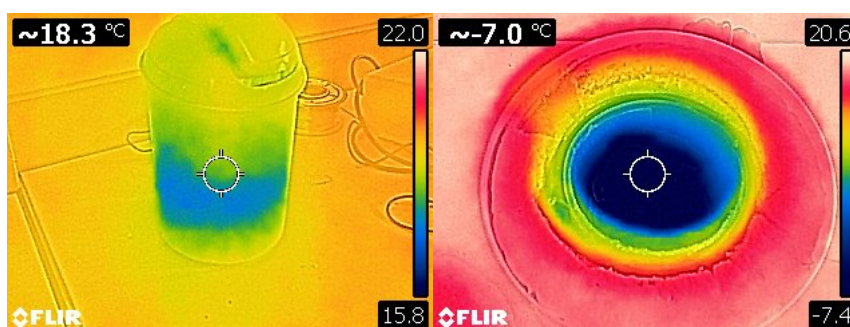
Figure 8. Temperature measurements inside and outside the small waste bin insulated at the end of the experiment (7 hours afterward) Figure left: heat flow from outside. Figure Right: heat flow inside.

During the experiment, ice storage was performed in the thermally insulated cylinder compartment to verify that the system could sustain the heat flux from the ice cubes at 0°C (cold source). The ice solids were retained within the enclosed adiabatic system for seven hours (refer to Figure 9). The results show that the system maintained the ice's temperature correctly (See Figure 9), with only 1°C lost during this period.

3.5.2. Hot Source Verification Test

The Steel wool filament (see Figure 4) produces heat using an AC generator with a maximal output of 33.93 watts (12.96 to 33.93 watts). The power in issue controls the heat flux through the samples.
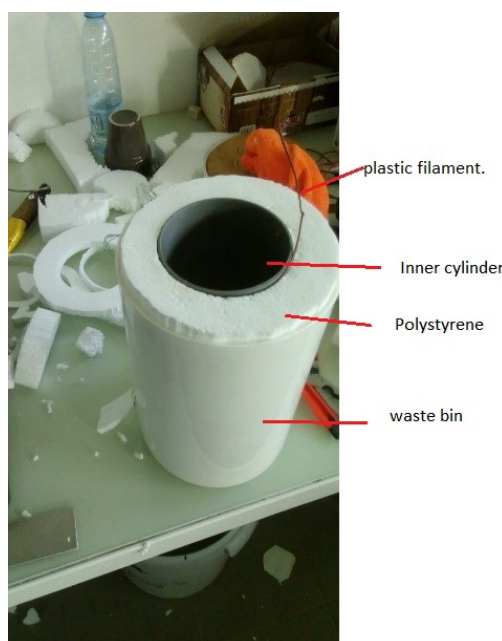
Figure 9. Adiabatic compartment of the calorimeter

Several tests (see Figure 10) were carried out to know the necessary power required for reaching 373.15 K (a further range is not pertinent to this experiment) without steel iron filament (see Figure 4) breaking. The experimental results are given in Table 1. The experimentation is conducted for the following three reasons:

- Determining the optimal power level that would permit heat transfer into the tested material without causing it to catch fire;
- ensuring that temperatures can be raised to 373.15 Kelvin and determining the precise power value necessary to achieve this temperature at the hot source; and

- And lastly, ensure that applying a current does not cause the iron filament to break (excessive power circulating through the filament may cause the cable to fuse). Following a series of experiments, it was determined that the ideal nominal power value is 33.9 W.
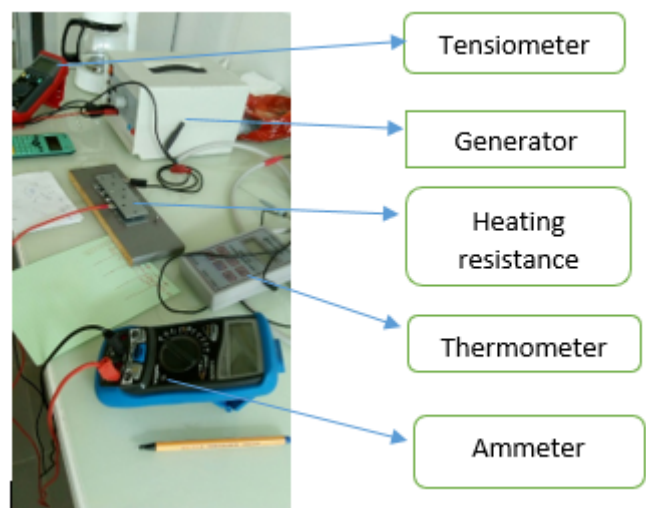
Figure 10. Calibration test of the hot source

Table 1. Power values obtained in the test of the hot source

The results of the Test (maximum power)				
	Intensities (A)	Voltages (V)	Temperature (K)	Power (W)
1	6	2.16	335.15	12.96
2	7.77	3	364.15	23.31
3	8.7	3.9	373.15	33.93

3.5.3. Thermocouple Calibrations

A LAUDA thermostat (model RE 104) was employed to calibrate the thermocouples Type T (see Figure 11) used during the experiments (refer to Appendix A for further details). Figure 12 illustrates the calibration results of some thermocouples. global relative error of each thermocouple don't exceed 0.90%.

Figure 11. Acquisition chain (see Appendix B for more information about the datalogger CR3000) of the thermocouples Type T test calibration

Figure 12. Example of calibration thermocouples
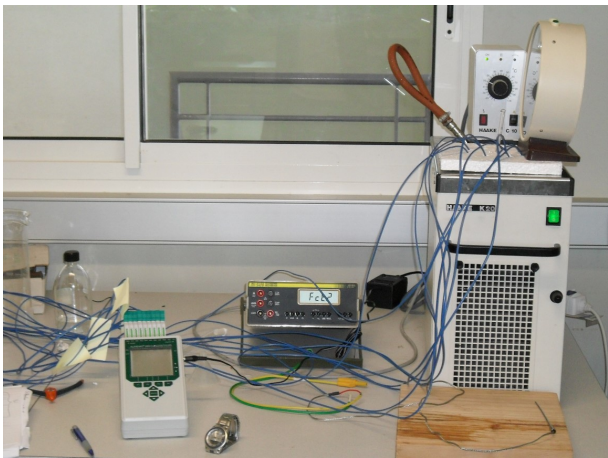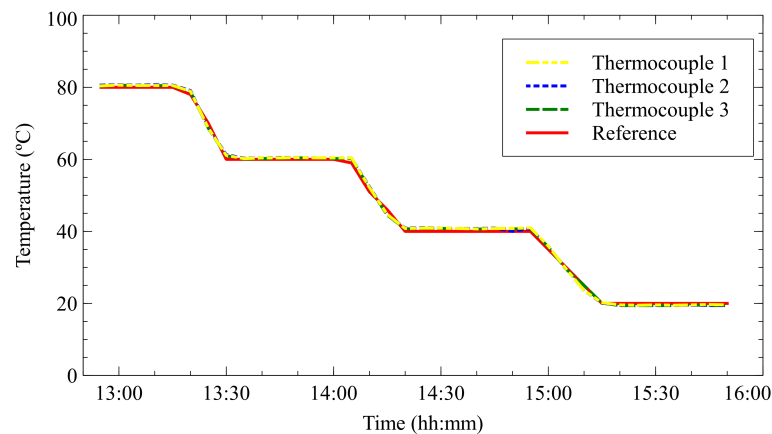
3.5.4. Protocol of Measurements

The sample is positioned in the intermediate space between two metallic cylinders (refer to Figure 4). The cold and hot sources, represented respectively by ice cubes and steel wool filament crossed by a current, are positioned opposite each other on the two metals, as illustrated in Figures 13 and 14. The thermal equilibrium state (i.e., steady state) is reached after 40 minutes. Four thermocouples, denoted as T_0, T_1, T_2 and T_3, are positioned intermediately among the various materials (for their respective positions, refer to Figure 13). The measurements collected are taken at one-minute intervals and then averaged over 40 minutes. The measurements are conducted three times to ensure that the results are reliable. The measurement acquisition chain, encompassing the construction of the calorimeter, utilization of type T thermocouples, use of connection cables, and data acquisition system (or datalogger) employed, conforms to the ASTM E1225 standard (i.e., the global error measurement does not exceed 5%). For more information about the error value, see the technical note of the ASTM International [45].
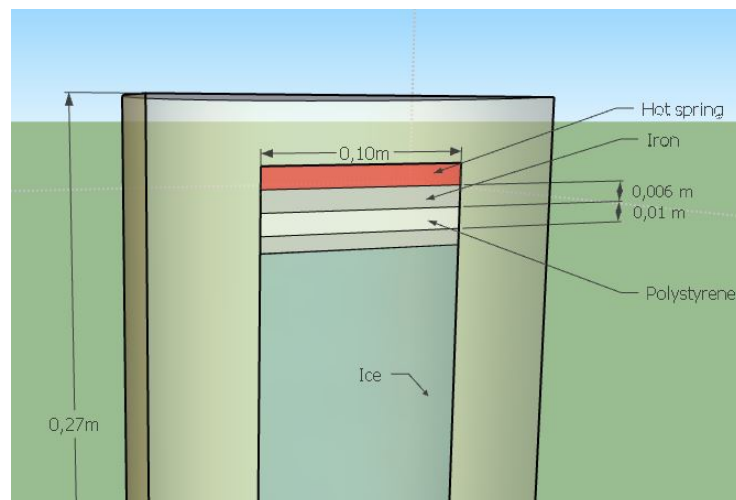

Figure 13. Position of the steel iron, sample (i.e., polystyrene for example), ice cubes and hot spring (i.e., steel wool filament) in the calorimeter box.
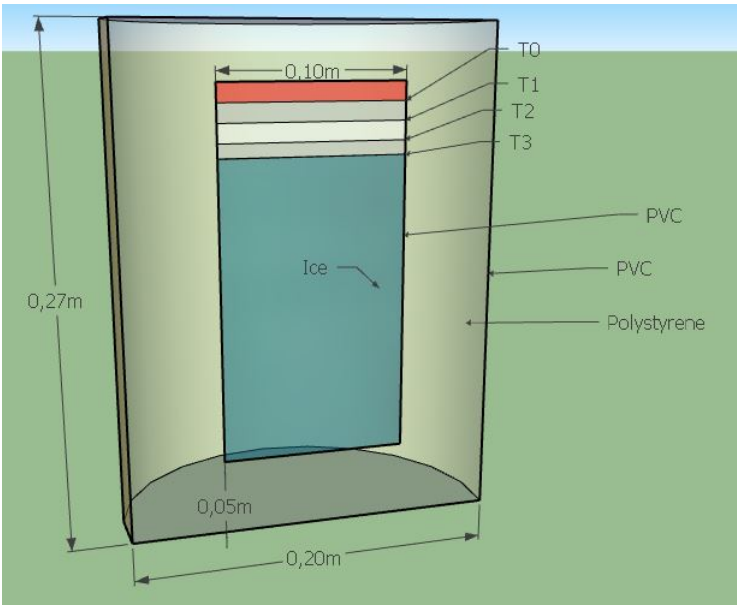
Figure 14. A representative cross-section of the different thermocouple positions used in the device.

4. Cost Price of the Device

Most materials used to construct the experimental device described in this work can be recycled, and all the materials are readily available around us. If they were to be purchased, the overall financial cost of these materials would amount to approximately 94.30 € (see Table 2 for the specification price). Since the data acquisition unit is the most expensive device, replacing it with a multi-meter is possible. In this case, the Thermocouples can be calibrated using the voltage signal they deliver, which is read directly on the voltmeter. The cost of a voltmeter of higher accuracy is approximately 100 €.

Table 2. Manufacturing price of the device (estimation price on Reunion Island for the year 2021-2022).

| N | Designation | Q | Dimensions | | Unit cost (€) | Total cost (€) |
			e (m)	dia (m)		
1	Generator	1			63	63
2	Steel wool	1			0.50	0.50
3	Thermocouple	4	0.018	0.1	4.20	16.80
4	Black flat steel iron	2	0.006	0.1	0	0
5	Polystyrene (sample)	1	0.01	0.1	0	0
6	Small waste bin	1	0.2	0.1	2	2
7	Ice	1			0	0
8	recycled Polystyrene (Isolation)	1			0	0
9	Tube PVC	1	0.002	0.1	1	1
10	Plug PVC	1	0.02	0.18	11	11
					Total	94.30 €

5. Results and Discussion

Three samples with known thermal conductivity (manufacturer data) were tested using the prototype designed: polystyrene, hard foam, and chipboard wood. The work was aims to verify the reliability of the experiment device to measure the thermal conductivity of the samples. Table 3 summary the results obtained. The mean thermal conductivity values collected from each sample during the experiment represent the experimental values provided by the device for each sample. By comparing the measured and reference values for the three samples, which should not exceed an acceptable error of 5%, it is reasonable to conclude that the device is functioning correctly. Further analysis of the curve related to the material under investigation, particularly polystyrene (i.e., which

exhibited the highest error during the experiment), reveals an absolute error value of approximately 0.0012 $W.m^{-1}\ K^{-1}$. This relative error value (i.e., 4%) confirms the device's measurement accuracy.

Table 3. Experimental (measurement) vs. theoretical (reference) thermal conductivity values.

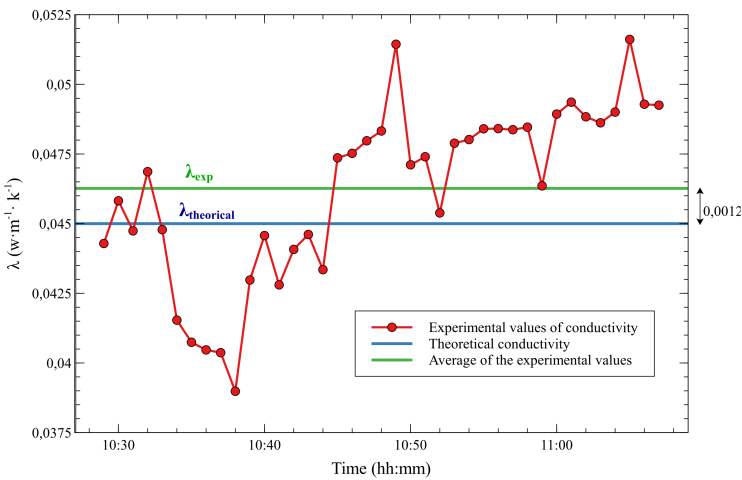| Type of materials	$\lambda_{theoretical}$ $(W.m^{-1}.K^{-1})$	λ_{exp} $(W.m^{-1}.K^{-1})$	Relative error
Hard foam	0.16	0.155	3.13 %
Polystyrene	0.045	0.0468	4 %
Chipboard wood	0.12	0.117	2.5 %

Figure 15. Comparison of the average experimental thermal conductivity value λ_{exp} of the polystyrene sample with the reference value (i.e., theoretical) $\lambda_{theoretical}$ (given by the manufacturer).

6. Conclusions

Experimental research poses a significant challenge for developing countries, often due to the prohibitively high costs of acquiring the necessary measuring equipment for conducting such experiments. The field of civil engineering is no exception to this challenge. This study proposed an experimental device capable of measuring an opaque and homogeneous material's thermal conductivity. This eco-designed and highly reliable device perfectly meets researchers' expectations in developing countries. Indeed, it offers the following advantages: it is easy to manufacture (i.e., reproducible), very cost-effective, and user-friendly. Measurements on reference material samples were conducted to ensure the device's reliability. The test results demonstrate that the machine can accurately determine the average values of the thermal conductivity of a construction material by ASTM E1225 Standard (see [45]). The prospects of this work would involve conducting studies to enhance the apparatus for accurately measuring thermal conductivity in non-homogeneous and non-opaque building materials, such as reflective thin products, phase change materials, translucent materials, or chromatic materials. The apparatus would also need to characterise the thermal conductivity of innovative next-generation materials already in the construction market.

Appendix A. Specifications thermostat RE104

RE104		
Operating temperature range	° C	-10 to 120
Ambient temperature range	° C	5 ... 40
Setting resolution	° C	0.1
Indication resolution	° C	0.1
Heater power 230 V; 50/ 60 Hz	kw	1.5
Heater power 115 V; 60 Hz		1.3
Heater power 100 V; 50/60 Hz		1.0
Pump type		pressure pump with choice of 5 output steps
Max. discharge pressure	bar	0.4
Max. flow rate	l/mm	17
Pump Connections	mm	nipples 13 mm dia.
Max. bath volume	l	3 to 4.5
Bath opening (W x D)	mm	130 x 105
Bath depth	mm	160
Usable depth	mm	140
Height top edge of bath	mm	363
Overall size (W x D x H)	mm	180 x 320 x 254
Weight	kg	21
Power consumption 230 V; 50/ 60Hz	KW	1.7
Power consumption 115 V; 60 Hz		1.4
Power consumption 100 V; 50/60 Hz		1.1
Safety features		FL
Temperature Control	$\pm$ ° C	0.05

Appendix B. Specifications Datalogger CR3000

Specifications CR3000	
-NOTE-	Note: Additional specifications are listed in the CR3000 Specifications Sheet.
Operating Temperature Range	-25° to +50° C (standard)-40° to +85°C (extended)Non-condensing environment
	The rechargeable base option has an operating temperature range of -40° to +60°C.
	The alkaline base option has a temperature range of -25° to +50°C.
	25° to +50°C (standard)-40° to +85°C (extended)
Analog Inputs	28 single-ended or 14 differential (individually configured)
Pulse Counters	4
Voltage Excitation Terminals	4 (VX1 to VX4)
Communications Ports	CS I/O
	RS-232
	Parallel peripheral
Switched 12 Volt	2 terminals
Digital I/O	Certain digital ports can be used to count switch closures.
	3 SDM and 8 I/Os or 4 RS-232 COM I/O
Input Limits	± 5 Vdc
Analog Voltage Accuracy	$\pm$ (0.04 % of reading + offset) at 0°to 40° C
ADC	16-bit
Power Requirements	10 to 16 Vdc
Real-Time Clock Accuracy	± 3 min. per year (Correction via GPS optional.)
Internet Protocols	FTP, HTTP, XML POP3, SMTP, Telnet, NTCIP, NTP,
Communication Protocols	PakBus, Modbus, DNP3, SDI-12, SDM
Warranty	3 years
Idle Current Drain, Average	2 mA (@ 12 Vdc)
Active Current Drain, Average	3 mA (1 Hz sample rate @ 12 Vdc without RS-232 communication)
	10 mA (100 Hz sample rate @ 12 Vdc without RS-232 communication)
	38 mA (100 Hz sample rate @ 12 Vdc with RS-232 communication)

Nomenclature

The following nomenclature are used in this manuscript:

T_0	Hot source thermocouple measurement (in K)
T_1	The Thermocouple that measures the sample's heated surface temperature (in K).
T_2	The Thermocouple that measures the sample's cooled surface temperature (in K).
T_3	Cold source thermocouple measurement (in K).
T_i	Surface temperature of any material (in K).
ϕ	Constant thermal flux crossing an opaque wall (in W).
$\phi_d esc$	Downward thermal flux through the experimental setup (in W).
$\phi_t rans$	Thermal flux passing horizontally through the experimental setup (in W).
e	Thickness of any material described in the Table 2 (in m).
dia	diameter of any material described in the Table 2 (in m).
A_0	Surface of the plate steel iron (in m^2).
A_x	Surface of the sample study (in m^2) .
d_0	Thickness of the plate steel iron (in m).
d_x	Thickness of the sample study (in m).
Plate A	Top plate steel iron (-).
Plate B	the sample plate study (-).
Plate C	Bottom plate steel iron (-).
ASTM	American Society for Testing and Materials.
TPS	Transient Plane Source measurement method.
HFM	"Hot Flow Meter" Method for measuring the thermal conductivity of a material (-).
GHF	"Guarded Heat Flow" Method for measuring the thermal conductivity of a material (-).
GHP	"Guarded Hot Plate" Method for measuring the thermal conductivity of a material (-).
GHB	"Guarded Hot Box" Method for measuring the thermal conductivity of a material (-).
IRT	"Infrared Thermography" Method for measuring the thermal conductivity of a material (-).
SHB	"Surface Heat Balance" Method for measuring the thermal conductivity of a material (-).
TBM	"Temperature Based Method" for measuring the thermal conductivity of a material (-).
TCB	"Transient-Cylinder Bridge" Method for measuring the thermal conductivity of a material (-).
P	Power delivered by the generator (in W).
U	Voltage delivered by the generator (in V).
I	Intensity delivered by the generator (in A).
α	Phase angle between current and voltage (in °).
$\lambda_e xp$	Thermal conductivity of the experimental sample measuring in the device (in $W.m^{-1}.K^{-1}$).
$\lambda_t heoretical$	Thermal conductivity reference of the sample giving by the manufacturer (in $W.m^{-1}.K^{-1}$).

References

1. Asadi, I.; Shafigh, P.; Hassan, Z.F.B.A.; Mahyuddin, N.B. Thermal conductivity of concrete–A review. *Journal of Building Engineering* **2018**, *20*, 81–93. https://doi.org/10.1016/j.jobe.2018.07.002.

2. Gomes, M.G.; Flores-Colen, I.; Da Silva, F.; Pedroso, M. Thermal conductivity measurement of thermal insulating mortars with EPS and silica aerogel by steady-state and transient methods. *Construction and Building Materials* **2018**, *172*, 696–705. https://doi.org/10.1016/j.conbuildmat.2018.03.162.

3. Boudenne, A.; Ibos, L.; Gehin, E.; Candau, Y. A simultaneous characterization of thermal conductivity and diffusivity of polymer materials by a periodic method. *Journal of Physics D: Applied Physics* **2003**, *37*, 132. https://doi.org/10.1088/0022-3727/37/1/022.

4. Hu, R.; Ma, A.; Li, Y. Transient hot strip measures thermal conductivity of organic foam thermal insulation materials. *Experimental Thermal and Fluid Science* **2018**, *91*, 443–450. https://doi.org/10.1016/j.expthermflusci.2017.10.038.

5. Cesaratto, P.G.; De Carli, M. A measuring campaign of thermal conductance in situ and possible impacts on net energy demand in buildings. *Energy and Buildings* **2013**, *59*, 29–36. https://doi.org/10.1016/j.enbuild.2012.08.036.

6. Cuce, E.; Cuce, P.M.; Guclu, T.; Besir, A.; Gokce, E.; Serencam, U. A novel method based on thermal conductivity for material identification in scrap industry: An experimental validation. *Measurement* **2018**, *127*, 379–389. https://doi.org/10.1016/j.measurement.2018.06.014.

7. Kim, K.H.; Jeon, S.E.; Kim, J.K.; Yang, S. An experimental study on thermal conductivity of concrete. *Cement and concrete research* **2003**, *33*, 363–371. https://doi.org/10.1016/S0008-8846(02)00965-1.

8. Guo, L.; Guo, L.; Zhong, L.; Zhu, Y. Thermal conductivity and heat transfer coefficient of concrete. *Journal of Wuhan University of Technology-Mater. Sci. Ed.* **2011**, *26*, 791–796. https://doi.org/10.1007/s11595-011-0312-3.

9. Desogus, G.; Mura, S.; Ricciu, R. Comparing different approaches to in situ measurement of building components thermal resistance. *Energy and Buildings* **2011**, *43*, 2613–2620. https://doi.org/10.1016/j.enbuild.2011.05.025.

10. Ahmad, A.; Maslehuddin, M.; Al-Hadhrami, L.M. In situ measurement of thermal transmittance and thermal resistance of hollow reinforced precast concrete walls. *Energy and Buildings* **2014**, *84*, 132–141. https://doi.org/10.1016/j.enbuild.2014.07.048.

11. Cesaratto, P.G.; De Carli, M.; Marinetti, S. Effect of different parameters on the in situ thermal conductance evaluation. *Energy and buildings* **2011**, *43*, 1792–1801. https://doi.org/10.1016/j.enbuild.2011.03.021.

12. Asdrubali, F.; Baldinelli, G. Thermal transmittance measurements with the hot box method: Calibration, experimental procedures, and uncertainty analyses of three different approaches. *Energy and buildings* **2011**, *43*, 1618–1626. https://doi.org/10.1016/j.enbuild.2011.03.005.

13. Zhu, X.; Li, L.; Yin, X.; Zhang, S.; Wang, Y.; Liu, W.; Zheng, L. An in-situ test apparatus of heat transfer coefficient for building envelope. *Building Energy Efficient* **2012**, *256*, 57–60.

14. Albatici, R.; Tonelli, A.M.; Chiogna, M. A comprehensive experimental approach for the validation of quantitative infrared thermography in the evaluation of building thermal transmittance. *Applied energy* **2015**, *141*, 218–228. https://doi.org/10.1016/j.apenergy.2014.12.035.

15. Fokaides, P.A.; Kalogirou, S.A. Application of infrared thermography for the determination of the overall heat transfer coefficient (U-Value) in building envelopes. *Applied energy* **2011**, *88*, 4358–4365. https://doi.org/10.1016/j.apenergy.2011.05.014.

16. Barreira, E.; Almeida, R.; Delgado, J. Infrared thermography for assessing moisture related phenomena in building components. *Construction and building materials* **2016**, *110*, 251–269. https://doi.org/10.1016/j.conbuildmat.2016.02.026.

17. Evangelisti, L.; Guattari, C.; Gori, P.; De Lieto Vollaro, R. In situ thermal transmittance measurements for investigating differences between wall models and actual building performance. *Sustainability* **2015**, *7*, 10388–10398. https://doi.org/10.3390/su70810388.

18. Nardi, I.; Ambrosini, D.; de Rubeis, T.; Sfarra, S.; Perilli, S.; Pasqualoni, G. A comparison between thermographic and flow-meter methods for the evaluation of thermal transmittance of different wall constructions. In Proceedings of the Journal of Physics: Conference Series. IOP Publishing, 2015, Vol. 655, p. 012007. https://doi.org/10.1088/1742-6596/655/1/012007.

19. Nardi, I.; Paoletti, D.; Ambrosini, D.; De Rubeis, T.; Sfarra, S. U-value assessment by infrared thermography: A comparison of different calculation methods in a Guarded Hot Box. *Energy and Buildings* **2016**, *122*, 211–221. https://doi.org/10.1016/j.enbuild.2016.04.017.

20. Glavaš, H.; Hadzima-Nyarko, M.; Haničar Buljan, I.; Barić, T. Locating hidden elements in walls of cultural heritage buildings by using infrared thermography. *Buildings* **2019**, *9*, 32. https://doi.org/10.3390/buildings9020032.

21. Evangelisti, L.; Scorza, A.; De Lieto Vollaro, R.; Sciuto, S.A. Comparison between heat flow meter (HFM) and thermometric (THM) method for building wall thermal characterization: latest advances and critical review. *Sustainability* **2022**, *14*, 693. https://doi.org/10.3390/su14020693.

22. Yüksel, N. The Review of Some Commonly Used Methods and Techniques to Measure the Thermal Conductivity of Insulation Materials. In *Insulation Materials in Context of Sustainability*; IntechOpen, 2016. https://doi.org/10.5772/64157.

23. Rausch, M.H.; Krzeminski, K.; Leipertz, A.; Fröba, A.P. A new guarded parallel-plate instrument for the measurement of the thermal conductivity of fluids and solids. *International Journal of Heat and Mass Transfer* **2013**, *58*, 610–618. https://doi.org/10.1016/j.ijheatmasstransfer.2012.11.069.

24. Chen, F.; Wittkopf, S.K. Summer condition thermal transmittance measurement of fenestration systems using calorimetric hot box. *Energy and Buildings* **2012**, *53*, 47–56. https://doi.org/10.1016/j.enbuild.2012.07.005.

25. Meng, X.; Gao, Y.; Wang, Y.; Yan, B.; Zhang, W.; Long, E. Feasibility experiment on the simple hot box-heat flow meter method and the optimization based on simulation reproduction. *Applied Thermal Engineering* **2015**, *83*, 48–56. https://doi.org/10.1016/j.applthermaleng.2015.03.010.

26. Meng, X.; Luo, T.; Gao, Y.; Zhang, L.; Shen, Q.; Long, E. A new simple method to measure wall thermal transmittance in situ and its adaptability analysis. *Applied Thermal Engineering* **2017**, *122*, 747–757. https://doi.org/10.1016/j.applthermaleng.2017.05.074.

27. Osaze, O.; Khanna, S. Experimental Thermal Conductivity Measurement of Hollow-Structured Polypropylene Material by DTC-25 and Hot Box Test. *Buildings* **2023**, *13*, 3094. https://doi.org/10.3390/buildings13123094.

28. Kurpińska, M.; Karwacki, J.; Maurin, A.; Kin, M. Measurements of thermal conductivity of LWC cement composites using simplified laboratory scale method. *Materials* **2021**, *14*, 1351. https://doi.org/10.3390/ma14061351.

29. Mobaraki, B.; Komarizadehasl, S.; Castilla Pascual, F.J.; Lozano-Galant, J.A.; Porras Soriano, R. A novel data acquisition system for obtaining thermal parameters of building envelopes. *Buildings* **2022**, *12*, 670. https://doi.org/10.3390/buildings12050670.

30. Biljana S. Vučićević, Valentina M. Turanjanin, V.V.B.M.P.J.S. Experimental and numerical modeling of thermal performance of a residential building in belgrade. *Thermal Science* **2009**, *13*, 245–252. https://doi.org/10.2298/TSCI0904245V.

31. Andargie, M.S.; Azar, E. An applied framework to evaluate the impact of indoor office environmental factors on occupants' comfort and working conditions. *Sustainable cities and society* **2019**, *46*, 101447. https://doi.org/10.1016/j.scs.2019.101447.

32. Evangelisti, L.; Guattari, C.; Gori, P.; de Lieto Vollaro, R.; Asdrubali, F. Experimental investigation of the influence of convective and radiative heat transfers on thermal transmittance measurements. *International Communications in Heat and Mass Transfer* **2016**, *78*, 214–223. https://doi.org/10.1016/j.icheatmasstransfer.2016.09.008.

33. Ricklefs, A.; Thiele, A.M.; Falzone, G.; Sant, G.; Pilon, L. Thermal conductivity of cementitious composites containing microencapsulated phase change materials. *International journal of heat and mass transfer* **2017**, *104*, 71–82. https://doi.org/10.1016/j.ijheatmasstransfer.2016.08.013.

34. Lucchi, E.; Roberti, F.; Alexandra, T. Definition of an experimental procedure with the hot box method for the thermal performance evaluation of inhomogeneous walls. *Energy and Buildings* **2018**, *179*, 99–111. https://doi.org/10.1016/j.enbuild.2018.08.049.

35. Gagliano, A.; Cascone, S. Eco-friendly green roof solutions: Investigating volcanic ash as a viable alternative to traditional substrates. *Construction and Building Materials* **2024**, *411*, 134442. https://doi.org/10.1016/j.conbuildmat.2023.134442.

36. Cuce, E.; Cuce, P.M.; Guclu, T.; Besir, A.; Gokce, E.; Serencam, U. A novel method based on thermal conductivity for material identification in scrap industry: An experimental validation. *Measurement* **2018**, *127*, 379 – 389. https://doi.org/https://doi.org/10.1016/j.measurement.2018.06.014.

37. Hu, R.; Ma, A.; Li, Y. Transient hot strip measures thermal conductivity of organic foam thermal insulation materials. *Experimental Thermal and Fluid Science* **2018**, *91*, 443 – 450. https://doi.org/https://doi.org/10.1016/j.expthermflusci.2017.10.038.

38. Gomes, M.G.; Flores-Colen, I.; da Silva, F.; Pedroso, M. Thermal conductivity measurement of thermal insulating mortars with EPS and silica aerogel by steady-state and transient methods. *Construction and Building Materials* **2018**, *172*, 696 – 705. https://doi.org/https://doi.org/10.1016/j.conbuildmat.2018.03.162.

39. Boudenne, A.; Ibos, L.; Géhin, E.; Candau, Y. A simultaneous characterization of thermal conductivity and diffusivity of polymer materials by a periodic method. *Journal of Physics D: Applied Physics* **2003**, *37*, 132. https://doi.org/10.1088/0022-3727/37/1/022.

40. Platzer, N. Encyclopedia of Polymer Science and Engineering, H. F. Mark, N. M. Bikales, C. G. Overberger, and G. Menges, Wiley-Interscience, New York, 1985, 720 pp. *Journal of Polymer Science Part C: Polymer Letters* **1986**, *24*, 359–360, [https://onlinelibrary.wiley.com/doi/pdf/10.1002/pol.1986.140240720]. https://doi.org/10.1002/pol.1986.140240720.

41. Mottram.; Taylor. Thermal transport properties. *international encyclopaedia of composity* **1989**, *127*, 379 – 389. https://doi.org/https://doi.org/10.1016/j.measurement.2018.06.014.

42. Fakra, D.A.H.; José, B.R.A.; Murad, N.M.; Gatina, J.C. A new affordable and quick experimental device for measuring the thermo-optical properties of translucent construction materials. *Journal of Building Engineering* **2020**, *32*, 101708. https://doi.org/10.1016/j.jobe.2020.101708.

43. Fakra, D.A.H.; José, B.R.A.; Murad, N.M.; Randriantsoa, A.N.A.; Gatina, J.C. Experimental data and calibration processes to a new and simple device dedicated to the thermo-optical properties of a polycarbonate construction material. *Data in Brief* **2020**, *32*, 106289. https://doi.org/10.1016/j.dib.2020.106289.

44. Delort, M.; Fakra, D.; Malet-Damour, B.; Gatina, J.C. Measuring the uncertainty assessment of an experimental device used to determine the thermo-optico-physical properties of translucent construction materials. *Measurement Science and Technology* **2022**, *33*, 055007. https://doi.org/10.1088/1361-6501/ac407b.

45. ASTM International. Standard Test Method for Thermal Conductivity of Solids by Means of the Guarded-Comparative-Longitudinal Heat Flow Technique. Technical report ASTM E1225-13, American Society for Testing and Materials, 2013. 8 pp.